Computers, Materials & Continua CMC, vol.62, no.1, pp.443-458, 2020

Complexity Effective Frequency and Sidelink Synchronization Algorithm for LTE Device-to-Device Communication Systems

Yong-An Jung[1], Min-Goo Kang[2] and Young-Hwan You[1, *]

Abstract: Device-to-device (D2D) communication is considered as a major challenge in the long term evolution (LTE) network wherein devices directly communicate with each other. One of the key challenges in D2D sidelink is reliable and reduced-complexity synchronization. To address this issue, a computationally efficient sequential detection scheme for integer carrier frequency offset and sidelink identity is proposed in the LTE-D2D system. To perform the frequency offset detection without retrieving the sidelink identity, the conjugate relation between two primary sidelink synchronization sequences is exploited, which facilitates the detection tasks of frequency offset and sidelink identity to be decoupled. It is demonstrated from simulation results that the inherent property of the sidelink synchronization sequences is effectively used for joint detection of frequency offset and sidelink identity with significantly reduced complexity, compared to existing estimation schemes.

Keywords: Long term evolution, device-to-device communication, carrier frequency offset, sidelink identity, sidelink synchronization.

1 Introduction

Orthogonal frequency division multiplexing (OFDM) has been adopted for a number of commercial wireless applications, including the digital video broadcasting-terrestrial (DVB-T), the IEEE 802.11n wireless local area network (WLAN), and the long term evolution (LTE). The LTE has been standardized by the third generation partnership project (3GPP) to support high-speed data transmission and guarantee low delay [3GPP TS36.211 v8.5.0 (2009)]. Recently, cellular internet of things (IoT) solutions such as narrowband IoT and device-to-device (D2D) communications have been paid much attention as a new communication paradigm in existing and future cellular LTE networks [Li, Li and Sun (2019); Zhao, Wang and Zhong (2019); Li and Lv (2018)]. D2D communication is considered as a promising technology for various IoT domains such as smart home, industrial automation and control, remote manufacturing, and healthcare [Tastan (2019); Zhou, Wu, Chen et al. (2018); Saleem, Jangsher, Qureshi et al. (2018); Al-Turjman and Alturjman (2018); Sisinni, Saifullah, Han et al. (2018)]. In particular,

[1] Department of Computer Engineering, Sejong University, Seoul, Korea.

[2] Department of IT Contents, Hanshin University, Gyeonggi-do, Korea.

[*] Corresponding Author: Young-Hwan You. Email: yhyou@sejong.ac.kr.

IoT that enables machine-to-machine communication among industrial devices without the essential control of the centralized supervision is a prime enabler to facilitate the evolution of 5G cellular network [Sisinni, Saifullah, Han et al. (2018); Wang, Chang, Wang et al. (2018); Zhou, Dong, Ota et al. (2016); Yang, Zhang, Dai et al. (2017); Ali and Hamouda (2017)].

In the LTE-D2D network, it is a challenging task to maintain the synchronization especially for out-of-network coverage scenarios, wherein the D2D devices have to synchronize with each other. To this end, the D2D device has not only to estimate symbol timing offset (STO) and carrier frequency offset (CFO) but also to capture the sidelink identity [Golnari, Shabany, Nezamalhosseini et al. (2015); Berggren and Popovic (2015); Sriharsha, Dama and Kuchi (2017); Nassralla, Mansour and Jalloul (2016); Zhang, Liu and Long (2012); Morelli and Moretti (2016); Chu, Lai, Lan et al. (2014); Myung, Kang, Baek et al. (2014); Morelli and Moretti (2017)]. Toward this, a synchronization source user equipment (UE) periodically transmits two specified synchronization signals, named as primary sidelink synchronization signal (PSSS) and secondary sidelink synchronization signal (SSSS). Most of the existing synchronization schemes are designed for downlink (DL) detection and are not the best solution for sidelink synchronization, but they can be applied to the D2D scenarios [Berggren and Popovic (2015); Sriharsha, Dama and Kuchi (2017); Nassralla, Mansour and Jalloul (2016); Zhang, Liu, and Long (2012); Morelli and Moretti (2016); Chu, Lai, Lan et al. (2014)]. The sidelink identity is acquired by combining the set ID transmitted in the PSSS and the sidelink ID transmitted in the SSSS. The initial cell search procedure in LTE system generally involves three steps. During the first step of the procedure, the D2D device exploits the redundant cyclic prefix (CP) to find the fractional frequency offset (FFO) and initial STO [Golnari, Shabany, Nezamalhosseini et al. (2015); Berggren and Popovic (2015); Sriharsha, Dama and Kuchi (2017)]. In the second step, the PSSS is used to retrieve the set ID and detect integer frequency offset (IFO) [Nassralla, Mansour and Jalloul (2016); Zhang, Liu and Long (2012); Morelli and Moretti (2016); Chu, Lai, Lan et al. (2014)]. After the completion of this stage, the SSSS is identified to determine the frame boundary and the sidelink ID [Myung, Kang, Baek et al. (2014); Morelli and Moretti (2017)].

In Sriharsha et al. [Sriharsha, Dama, and Kuchi (2017); Nassralla, Mansour and Jalloul (2016); Zhang, Liu and Long (2012)], the PSSS detection method was proposed to be performed in the time domain. One drawback of this strategy is that the detection accuracy depends on the existence of the IFO. To solve this issue, various synchronization schemes have been presented by detecting the PSSS in the frequency domain [Zhang, Liu and Long (2012); Morelli and Moretti (2016); Chu, Lai, Lan et al. (2014)]. In Morelli et al. [Morelli and Moretti (2016)], IFO detection can be jointly accomplished during the PSSS-matching phase, which is based on differential correlation method that involves a huge number of arithmetic operations. To reduce the computational load, a sequential IFO and set ID estimation scheme has been presented exploiting the symmetric property of the PSSS [Chu, Lai, Lan et al. (2014)]. This approach suffers from the presence of residual STO, degrading its detection efficiency. Thus, it is of significant interest to develop reliable synchronization method while reducing hardware complexity and power consumption of D2D devices.

In this paper, a computationally efficient IFO and set ID detection scheme is proposed for the LTE-D2D communication. The conjugate property in the PSSS sequence facilitates the detection of the IFO without relying on the set ID, which enables a joint detection of the IFO and set ID to be decoupled into two sequential detection tasks. Numerical analysis is performed to present the relationship between detection probability and design parameter. It is demonstrated through numerical simulations that the proposed scheme does not have a significant computational complexity and is easy to implement, while offering moderate performance when compared to conventional algorithms.

The reminder of this paper is structured as follows. Next section describes the system model and synchronization signal used in this paper. In Section 3, the conventional non-coherent estimation schemes are presented using differential correlation. Section 4 proposes a reduced-complexity and sequential detection scheme in the LTE-D2D system. In Section 5, the performance of the proposed detection scheme is demonstrated by computer simulations. Finally, conclusions are drawn in Section 6.

2 System descriptions

2.1 Signal model

Consider an OFDM system that employs N non-zero subcarriers and N_g guard interval (GI) samples whose durations are T and T_g, respectively. After taking an N-point inverse fast Fourier transform (IFFT) on the information symbols, a CP is added at the head of OFDM symbol to remove inter-symbol interference (ISI) caused by STO, creating one effective OFDM symbol $x_q(v)$ over the q-th duration. Mathematically, one OFDM symbol $x_q(v)$ can be written by

$$x_q(v) = \sum_{k=-N/2}^{N/2-1} X_q(k) e^{j2\pi kv/N}, v = -N_g, -N_g+1, \cdots, N-1 \quad (1)$$

where v denotes the discrete time index and $X_q(k)$ is the frequency-domain signal at the k-th subcarrier during the q-th period.

Since the FFO marginally affects the performance of the IFO detection scheme like the existing approaches [Morelli and Moretti (2016); Chu, Lai, Lan et al. (2014)], it is assumed that the FFO is successfully removed at the receiver. After FFO compensation, the symbol timing is recovered to remove the GI. We assume that there is a residual STO τ due to the presence of highly dispersive channels [Golnari, Shabany, Nezamalhosseini et al. (2015)]. Without losing generality, we consider only integer-valued τ because any fractional STO can be incorporated into the channel impulse response (CIR). In the presence of the STO τ, the sampling of OFDM symbol q is shifted from the optimal position and done at time instants $t = qT_u + vT_s + \tau T_s$, where $T_u = T + T_g$ and T_s is the sampling interval satisfying the Nyquist rate. Thus, the time-domain signal during the q-th period $y_q(v)$, $v = -N_g, -N_g+1, \cdots, N-1$, appears as Nassralla et al. [Nassralla, Mansour and Jalloul (2016)]

$$y_q(v) = e^{jq\epsilon N_g \rho} e^{j\epsilon(v-\tau)\rho} \sum_{p=1}^{L} h_q(p) x_q(v-\tau_p-\tau) + z_q(v) \tag{2}$$

where $\rho = 2\pi / N$, ϵ denotes the normalized IFO with respect to the subcarrier spacing $\Delta f = 1/(NT_s)$, $h_q(p)$ is the discrete CIR with L resolvable paths, τ_p is the delay of the p-th path, and $z_q(v)$ is the contribution of a zero-mean additive white Gaussian noise (AWGN). Extracting the CP and performing the FFT, the frequency-domain signal in the k-th subcarrier over the q-th period suffering from the IFO can be given by Morelli et al. [Morelli and Moretti (2016)]

$$Y_q(k) = H_q(k-\epsilon) X_q(k-\epsilon) e^{-j(k-\epsilon)\tau\rho} e^{jq\epsilon N_g \rho} + Z_q(k), \ |k| \le N_p/2 \tag{3}$$

where $H_q(k)$ is the frequency response of the channel, $Z_q(k)$ is a complex zero-mean AWGN having variance σ_Z^2, and N_p denotes the number of non-zero PSSS/SSSS subcarriers.

2.2 Synchronization signal

Level An LTE sidelink network can support 336 different sidelink identities indexed by $N_{ID} \in \{0,1,2,\cdots,335\}$, which are grouped into two sets $\{0,1,2,\cdots,167\}$ and $\{168,169,\cdots,335\}$. The set ID embedded in the PSSS indicates whether the UE is in coverage area or out of coverage area. The PSSS is chosen in a set of two different Zadoff-Chu (ZC) sequences with sequence index u_i $(i=0,1)$. A UE within the network coverage transmits PSSS symbols with index u_0, whereas a UE outside of the network coverage transmits PSSS symbols with index u_1. The PSSS sequence is mapped onto the 72 central subcarriers around DC, which consists of 62 plus 10 guard subcarriers, leading to $N_p = 62$ non-zero PSSS subcarriers with the center component being nulled to avoid transmission on DC subcarrier. Two PSSS sequences can be expressed as [3GPP TS36.211 v8.5.0. (2009)]

$$P_i(k) = \begin{cases} e^{-j\pi u_i(k+31)(k+32)/63}, & k \in \mathcal{P} \\ 0 & otherwise \end{cases} \tag{4}$$

where $\mathcal{P} = \{k \mid -N_p/2 \le k \le N_p/2, k \ne 0\}$. In the D2D sidelink, the ZC root sequence index $\{u_0, u_1\} = \{26, 37\}$ such that ZC sequences are complex conjugates of each other, namely, $P_0(k) = P_1^*(k)$.

The main usage of the SSSS is to retrieve the sidelink ID and to find the beginning point of an LTE frame. The SSSS is a frequency-domain binary phase-shift keying sequence, which is an interleaved combination of two length-31 scrambled maximum length sequences $s_{w_0}(u)$ and $s_{w_1}(u)$, with $u = 0,1,\cdots,N_p/2-1$. Therefore, the SSSS is given by

$$R(2u) = \begin{cases} s_{w_0}(u) r_0(u) & in\ subframe\ 0 \\ s_{w_1}(u) r_0(u) & in\ subframe\ 5 \end{cases} \tag{5}$$

and

$$R(2u+1) = \begin{cases} s_{w_1}(q) r_1(u) d_{w_0}(u) & in\ subframe\ 0 \\ s_{w_0}(q) r_1(u) d_{w_1}(u) & in\ subframe\ 5 \end{cases} \tag{6}$$

where $r_i(u)$ and $d_{w_i}(u)$ represent the scrambling sequences. The sequence $R(u)$ is mapped onto central N_p SSSS subcarriers with indices $k \in \mathcal{P}$. The PSSS and SSSS symbols are transmitted twice within the same subframe for a quick acquisition of the timing and frequency information, as well as the sidelink identifier.

A series of process of acquiring time and frequency synchronization is called as initial synchronization. To this end, the PSSS and SSSS sequences are periodically transmitted by a synchronization source UE. The D2D synchronization procedure mainly comprises three steps as shown in Fig. 1. In the first step, initial STO and FFO estimation is accomplished in the time domain by using redundant information from the CP. After FFO compensation and CP removal, the time-sampled OFDM signal is transformed to the frequency domain by means of a FFT. During the next stage, the set ID is retrieved together with the IFO by detecting the PSSS, which can be performed in the time or frequency domain. Once these two steps are completed, the frame boundary and the sidelink ID are identified by detecting the SSSS, thus recovering the radio frame timing for the D2D communication. Upon successful completion of initial synchronization, the UE is able to access important system information carried through physical broadcast channel, such as FFT size and CP length.

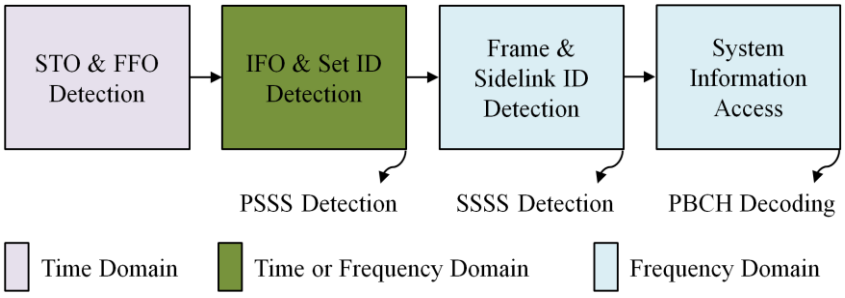

Figure 1: Initial synchronization procedure in the LTE-D2D system

3 Conventional estimation method

The IFO and set ID detection is typically performed in a non-coherent manner since the channel state information has not been known during the synchronization phase. For notational convenience, we consider the situation where the PSSS is transmitted on the l-th OFDM symbol with symbol energy $E_p = |P_i(k)|^2$, i.e. $X_l(k) = P_i(k)$. In order to

remove the effect of fading channel and STO, differential correlation between neighboring subcarriers can be performed as

$$\begin{aligned}\overline{Y}_l(k) &= Y_l(k)Y_l^*(k-1) \\ &= |H_l(k-\epsilon)|^2 D_i(k-\epsilon)e^{j\tau\rho} + \overline{Z}_l(k), k \in [-N_p/2+1,-1] \cup [2, N_p/2]\end{aligned} \tag{7}$$

where $(\cdot)^*$ means the complex conjugate, $D_i(k) = P_i(k)P_i^*(k-1)$ is the differential relation between two adjacent PSSS subcarriers, and $\overline{Z}_l(k)$ is a complex zero-mean noise contribution given by

$$\begin{aligned}\overline{Z}_l(k) &= H_l(k-\epsilon)X_l(k-\epsilon)Z_l^*(k-1)e^{-j(k-\epsilon)\tau\rho}e^{jl\epsilon N_g\rho} \\ &+ H_l^*(k-\epsilon-1)X_l^*(k-\epsilon-1)Z_l(k)e^{j(k-\epsilon)\tau\rho}e^{-jl\epsilon N_g\rho} + Z_l(k)Z_l^*(k-1).\end{aligned} \tag{8}$$

In this section, two conventional detection schemes using the differential correlation are briefly addressed. One is a reduced-complexity joint IFO and set ID detection (RCJD) method [Zhang, Liu and Long (2012); Morelli and Moretti (2016)] and the other is a sequential IFO and set ID detection (SISID) method [Chu, Lai, Lan et al. (2014)].

The RCJD scheme developed in Zhang et al. [Zhang, Liu, and Long (2012); Morelli and Moretti (2016)] is commonly used in the LTE system, which uses inherent central-symmetric characteristic of the ZC signals. In this scheme, the objective function $\Phi_a(m,n)$ can be expressed in terms of symmetric-conjugate differential correlation

$$\Phi_a(m,n) = \sum_{k\in\mathcal{D}} \left\{\overline{Y}_l(k+m) + \overline{Y}_l^*(-k+m+1)\right\} D_n^*(k) \tag{9}$$

where m is the hypothesized IFO and $\mathcal{D} \in [2, N_p/2]$. By finding the maximum of $\Phi_a(m,n)$ subject to m and n, the estimate of ϵ and n can be obtained by [Morelli and Moretti (2016)]

$$(\hat{\epsilon}, \hat{n}) = \arg\max_{m\in\mathcal{S}_f, n\in\mathcal{S}_i} \Phi_a^I(m,n) \tag{10}$$

where $(\cdot)^I$ denotes the real part of the enclosed quantity, $\mathcal{S}_i = \{0,1\}$, and $\mathcal{S}_f = \{-M, -M+1, \cdots, M\}$ for a nonnegative integer M. Note that M corresponds to the finite number of possibilities of ϵ depending on the oscillator's stability. Using the central-symmetric property of the ZC sequences, half-length complex correlation between the received ZC sequence and the original sequence can be performed. However, the RCJD scheme is still of considerable complexity.

In the SISID scheme, a normalized received PSSS is used to remove the effect of the channel fading, producing the channel-compensated objective function as given by

$$\Phi_b(m) = \frac{1}{N_p/2-1} \sum_{k\in\mathcal{D}} \tilde{Y}_l(k+m)\tilde{Y}_l(-k+m+1) \tag{11}$$

where $\tilde{Y}_l(k) = \overline{Y}_l(k)/|\overline{Y}_l(k)|$. By finding for the minimum of the cost function $\Phi_b(m)-1$, the estimate of ϵ can be obtained by

$$\epsilon = \arg\min_{m \in \mathcal{S}_f} \left| \Phi_b(m) - 1 \right|. \tag{12}$$

Since $\Phi_b(m)$ is independent of ZC index u_l, the estimation of the IFO and set ID is decoupled. Hence, the set ID is detected with one-dimensional search space as follows

$$\hat{n} = \arg\max_{n \in \mathcal{S}_i} \Phi_c^I(n) \tag{13}$$

where

$$\Phi_c(n) = \sum_{k \in \mathcal{D}} \{ \tilde{Y}_l(k + \epsilon) + \tilde{Y}_l^*(-k + \epsilon + 1) \} D_n^*(k). \tag{14}$$

The main drawback of the SISID method is that the impact of the STO on the detection performance is doubled in comparison with Eq. (10).

4 Proposed estimation methodμ

In this section, an effective sequential detection of the IFO and set ID is proposed exploiting the complex-conjugate feature of two PSSS signals in LTE-D2D systems. The differential correlation is adopted to compensate the effect of channel fading and then two complex-conjugate PSSS sequences are used to facilitate a reduced-complexity estimation. As a performance indicator, the probability of detection failure of the proposed sequential detection method is presented.

4.1 Algorithm description

For each IFO trial m, two possible $\Phi_a(m,n)$'s for $n = 0,1$ are averaged to remove the ambiguity of transmitted PSSS, which enables the IFO to be detected without the PSSS-matching process. With this concept in mind, the objective function is expressed using $\Phi_a(m,n)$

$$\Phi_d(m) = \frac{1}{2} \sum_{n=0}^{1} \Phi_a(m,n) \tag{15}$$

which is further derived as

$$\Phi_d(m) = \frac{1}{2} \sum_{k \in \mathcal{D}} \left\{ \bar{Y}_l(k + m) + \bar{Y}_l^*(-k + m + 1) \right\} \sum_{n=0}^{1} D_n^I(k). \tag{16}$$

It is worthy stating that $\Phi_d(m)$ is independent of ZC index u_n due to averaging $\Phi_a(m,n)$. Recalling from Eq. (4) that $P_0(k) = P_1^*(k)$, it is effortlessly seen that $D_0(k) = D_1^*(k)$. Using this complex-conjugate property, $\Phi_d(m)$ can be expressed in terms of $D_0(k)$

$$\Phi_d(m) = \sum_{k \in \mathcal{D}} \left\{ \bar{Y}_l(k + m) + \bar{Y}_l^*(-k + m + 1) \right\} D_0^I(k) \tag{17}$$

which indicates that the joint estimation for the IFO and set ID is decoupled.

Under the hypothesis that $m = \epsilon$ (hypothesis $\mathcal{H}_1$), substituting Eq. (7) into Eq. (17) gives

$$\Phi_d(m) = \sum_{k\in\mathcal{D}} |H_l(k)|^2 D_i(k) D_0^I(k) e^{j\tau\rho} + \sum_{k\in\mathcal{D}} |H_l(-k+1)|^2 D_i^*(-k+1) D_0^I(k) e^{-j\tau\rho} + \sum_{k\in\mathcal{D}} \hat{Z}_l(k) \tag{18}$$

where $\hat{Z}_l(k) = \{\overline{Z}_l(k) + \overline{Z}_l^*(-k+1)\} D_0^I(k)$. Thus, using the symmetric-conjugate relation $D_i(k) = D_i^*(-k+1)$, the real part of $\Phi_d(m)$ can be written by

$$\Phi_d^I(m) = \alpha \sum_{k\in\mathcal{D}} \{|H_l(k)|^2 + |H_l(-k+1)|^2\} |D_0^I(k)|^2 + \beta \sum_{k\in\mathcal{D}} \{|H_l(k)|^2 + |H_l(-k+1)|^2\} D_i^Q(k) D_0^I(k) + \sum_{k\in\mathcal{D}} \hat{Z}_l^I(k) \tag{19}$$

where $\alpha = \cos(\tau\rho)$ and $\beta = -\sin(\tau\rho)$. Under hypothesis that $m \neq \epsilon$ (hypothesis $\mathcal{H}_0$), $\Phi_d(m)$ can be expressed as

$$\Phi_d(m) = \sum_{k\in\mathcal{D}} |H_l(k+m-\epsilon)|^2 D_i(k+m-\epsilon) D_0^I(k) e^{j\tau\rho} + \sum_{k\in\mathcal{D}} |H_l(-k+1+m-\epsilon)|^2 D_i^*(-k+1+m-\epsilon) D_0^I(k) e^{-j\tau\rho} + \sum_{k\in\mathcal{D}} \hat{Z}_l(k). \tag{20}$$

Considering that $D_i(k)$'s are statistically independent for any i and k, the central limit theorem ensures that Eq. (20) is treated as a zero-mean Gaussian random variable. Consequently, the criterion for the IFO detection is constructed as

$$\hat{\epsilon} = \arg\max_{m\in\mathcal{S}_f} \Phi_d^I(m). \tag{21}$$

After the IFO detection, we select the largest metric of possible sets u_0 and u_1 as follows

$$\hat{n} = \arg\max_{n\in\mathcal{S}_i} \Phi_a^I(\hat{\epsilon}, n) \tag{22}$$

which can be equivalently performed by comparing $\Phi_a^I(\hat{\epsilon}, 0)$ and $\Phi_a^I(\hat{\epsilon}, 1)$

$$\Phi_a^I(\hat{\epsilon}, 0) \underset{u_0}{\overset{u_1}{\gtrless}} \Phi_a^I(\hat{\epsilon}, 1). \tag{23}$$

Using Eq. (9) and $D_0(k) = D_1^*(k)$, the hypothesis testing problem in Eq. (23) can be simplified to

$$\Phi_a^I(\hat{\epsilon}, 0) - \Phi_a^I(\hat{\epsilon}, 1) = \sum_{k\in\mathcal{D}} \hat{Y}_l^Q(k+\hat{\epsilon}) D_0^Q(k) \underset{u_0}{\overset{u_1}{\lessgtr}} 0 \tag{24}$$

where $\hat{Y}_l(k+\hat{\epsilon}) = \overline{Y}_l(k+\hat{\epsilon}) + \overline{Y}_l^*(-k+\hat{\epsilon}+1)$ and $(\cdot)^Q$ denotes the quadrature part of the enclosed complex number.

4.2 Performance analysis

The overall probability of detection failure, denoted as $P_f = Prob\{\epsilon \neq \epsilon, \hat{n} \neq i\}$, is used as a performance measure. In the non-fading channel, the overall probability of detection failure of the presented sequential estimation scheme is derived considering the situation where $\tau = 0$. Under hypothesis $\mathcal{H}_1$, $\Phi_d^I(m)$ is characterized by Gaussian distribution having mean $\mu_f = (N_p/2-1)E_P^2$ and variance $\sigma_{f1}^2 = (N_p/2-1)E_P^2(E_P\sigma_Z^2 + \sigma_Z^4/2)$. Under hypothesis $\mathcal{H}_0$, $\Phi_d^I(m)$ is regarded as a zero-mean Gaussian random variable having variance $\sigma_{f0}^2 = (N_p/2-1)E_P^4/2 + (N_p/2-1)E_P^2(E_P\sigma_Z^2 + \sigma_Z^4/2)$. Let $z = \Phi_d^I(m)$ be the real part of $\Phi_d(m)$ and $\gamma = E_P/\sigma_Z^2$ be the signal-to-noise ratio (SNR). If all the IFOs are equally likely to occur with a range $|\epsilon| \leq M$, the probability that the IFO is correctly recovered is calculated as

$$P_{d1} = \int_{-\infty}^{\infty} \frac{1}{\sqrt{2\pi}} e^{-\frac{z^2}{2}} \left[1 - Q\left(\frac{\sigma_{f1}}{\sigma_{f0}} z + \frac{\mu_f}{\sigma_{f0}}\right)\right]^{2M} dz \tag{25}$$

where $Q(\cdot)$ represents the Q-function,

$$\frac{\sigma_{f1}^2}{\sigma_{f0}^2} = \frac{1/\gamma + 1/2\gamma^2}{1/2 + 1/\gamma + 1/2\gamma^2} \tag{26}$$

and

$$\frac{\mu_f^2}{\sigma_{f0}^2} = \frac{N_p/2-1}{1/2 + 1/\gamma + 1/2\gamma^2}. \tag{27}$$

A closed-form approximation of Eq. (25) can be obtained by approximating Q-function by [Bao, Tuyen, and Tue (2014)]

$$Q\left(\frac{\sigma_{f1}}{\sigma_{f0}} z + \frac{\mu_f}{\sigma_{f0}}\right) \leq \lambda_0 e^{-\lambda_1\left(\frac{\sigma_{f1}}{\sigma_{f0}} z + \frac{\mu_f}{\sigma_{f0}}\right)} e^{-\lambda_2\left(\frac{\sigma_{f1}}{\sigma_{f0}} z + \frac{\mu_f}{\sigma_{f0}}\right)^2} \tag{28}$$

where $\lambda_0 = 0.49$, $\lambda_1 = 8/13$, and $\lambda_2 = 1/2$ are the fitting factors. Substituting Eq. (28) to Eq. (25) and using binomial expansion, a tight lower bound on P_{d1} can be obtained as

$$P_{d1} \geq \sum_{m=0}^{2M} (-\lambda_0)^m \binom{2M}{m} P_m \tag{29}$$

where

$$P_m = \frac{1}{\sqrt{2\pi}} \int_{-\infty}^{\infty} e^{-\frac{z^2}{2}} e^{-m\lambda_1\left(\frac{\sigma_{f1}}{\sigma_0} z + \frac{\mu_f}{\sigma_{f0}}\right)} e^{-m\lambda_2\left(\frac{\sigma_{f1}}{\sigma_0} z + \frac{\mu_f}{\sigma_{f0}}\right)^2} dz \tag{30}$$

which can be derived in a closed form [Gradshteyn and Ryzhik (2014)]

$$P_m = \left(1 + 2m\lambda_2 \frac{\sigma_{f1}^2}{\sigma_{f0}^2}\right)^{-1/2} e^{-\frac{\mu_f^2}{2\sigma_{f0}^2}} e^{\frac{1}{2}\left(\frac{\mu_f}{\sigma_{f0}} - m\lambda_1 \frac{\sigma_{f1}}{\sigma_{f0}}\right)^2 \left(1+2m\lambda_2 \frac{\sigma_{f1}^2}{\sigma_{f0}^2}\right)^{-1/2}}. \quad (31)$$

The correct detection probability conditioned on β can thus be lower-bounded as

$$P_{d1} \geq \sum_{m=0}^{2M} (-\lambda_0)^m \binom{2M}{m} \left(1 + 2m\lambda_2 \frac{\sigma_{f1}^2}{\sigma_{f0}^2}\right)^{-1/2} e^{-\frac{\mu_f^2}{2\sigma_{f0}^2}} e^{\frac{1}{2}\left(\frac{\mu_f}{\sigma_{f0}} - m\lambda_1 \frac{\sigma_{f1}}{\sigma_{f0}}\right)^2 \left(1+2m\lambda_2 \frac{\sigma_{f1}^2}{\sigma_{f0}^2}\right)^{-1/2}}. \quad (32)$$

When the received samples match with the PSSS, i.e. $n = i$, $\Phi_a^I(\epsilon, n)$ in Eq. (23) follows the Gaussian distribution with mean μ_s and variance σ_{s1}^2, while σ_{s0}^2 is the variance of a zero-mean Gaussian random variable $\Phi_a^I(\epsilon, n)$ under the condition when $n \neq i$. In such a case, the probability of correct set ID detection can be given by

$$P_{d2} = \int_{-\infty}^{\infty} \frac{1}{\sqrt{2\pi}} e^{-\frac{z^2}{2}} \left\lceil 1 - Q\left(\frac{\sigma_{s1}}{\sigma_{s0}} z + \frac{\mu_s}{\sigma_{s0}}\right) \right\rceil dz \quad (33)$$

which has a closed form expression

$$P_{d2} = 1 - Q\left(\frac{\mu_s}{\sqrt{\sigma_{s0}^2 + \sigma_{s1}^2}}\right) \quad (34)$$

where $\mu_s = 2\mu_f$, $\sigma_{s0}^2 = 2\sigma_{f0}^2$, and $\sigma_{s1}^2 = 2\sigma_{f1}^2$. Thus, the upper bound of the probability $P_f = Prob\{(\hat{\epsilon}, \hat{n}) \neq (\epsilon, i)\}$ can be obtained as $P_f \leq 1 - P_{d1} \times P_{d2}$.

4.3 Complexity analysis

The The complexity of the detection schemes is evaluated in terms of the number of real floating point operations (flops). For a fair complexity comparison, it is assumed that one complex multiplication, one complex addition, and one absolute operation correspond to six, two, and three real flops, respectively [Golub and Vanloan (1996)]. Furthermore, the quantity $D_n(k)$ has been assumed to be pre-calculated. To compute the shifted differential correlations $\overline{Y}_l(k+m)$ and $\overline{Y}_l(-k+m+1)$, it requires $N_p + 2M - 1$ complex multiplications for hypotheses $m \in \mathcal{S}_f$. We count only the number of flops used to calculate $\Phi_a^I(m,n)$ and $\Phi_c^I(n)$. In Eq. (9), $2N_p - 5$ flops are required to calculate $\Phi_a^I(m,n)$. Therefore, the overall number of flops needed to get Eq. (10) is $12M + 6N_p - 6 + (4M+2)(2N_p - 5)$. Since the absolute operation demands both real and imaginary parts of $\Phi_b(m)$, $8N_p - 13$ flops are required to get the metric $|\Phi_b(m) - 1|$ and then Eq. (12) requires $12M + 6N_p - 6 + (2M+1)(8N_p - 13)$ flops. Additionally, $6N_p - 14$ flops are required for $\Phi_c^I(n)$. In the case of the proposed scheme, Eq. (17)

requires $3N_p/2-4$ flops for each IFO trial and $3N_p/2-4$ flops are required in Eq. (24). Considering the range of IFO hypotheses, the number of total flops is $12M+6N_p-6+(2M+2)(3N_p/2-4)$.

5 Simulation results

The performance of the proposed sequential detector is evaluated using the system parameters designed for the LTE-D2D system with 5 MHz bandwidth and normal CP. The carrier center frequency is 2 GHz, the subcarrier spacing is Δf =15 kHz, the sampling time instant is, T_s =1/7.68 μs the FFT size is $N=512$, and the GI length is $N_g=128$. We adopt the Pedestrian A and Vehicular A channel models [ITU-R Recommendation M.1225]. Taking into consideration the low mobility and the stability of oscillators for D2D applications [Sexton, Bodinier, Farhang et al. (2018)], we set $M=2$ to have $\mathcal{S}_f=\{0,\pm1,\pm2\}$. The true set ID is generated randomly from $\mathcal{S}_i=\{0,1\}$ and integer-valued STO is generated uniformly from $[0,\tau_{max}]$, where τ_{max} is a maximum STO.

Fig. 2 presents the overall probability of detection failure in jointly detecting the IFO and set ID in the non-fading channel when $\tau_{max}=0$, i.e., in the case of perfect symbol timing recovery. It is observed that theoretical analysis (symbols) obtained using numerical integral exactly matches simulated results (lines) for the case of the RCJD and proposed schemes. A SNR loss of the proposed detection method over the RCJD scheme is about 2 dB because of the use of only real part of the PSSS in Eq. (17). As predicted, the performance of the detection schemes is degraded as the local oscillator's stability is getting worse, namely, M becomes larger.

Figs. 3 and 4 present the probabilities $Prob\{\epsilon\neq\epsilon\}$ and $Prob\{\hat{n}\neq i\}$, respectively. Consider the Pedestrian A and Vehicular A channel models, which are represented by a maximum excess delay of 0.41 μs and 2.15 μs, respectively. Here, the symbol timing error is set to two representative cases: $\tau_{max}=0$ and $\tau_{max}=20$. It is evident that the existence of frequency selectivity heavily affects the detection accuracy of the IFO and set ID recovery schemes in a severe multipath fading channel, wherein each subcarrier is subject to a different channel attenuation. On the other hand, the performance of the IFO detectors is more influenced by the amount of the STO than that of the set ID detectors. This phenomenon is more pronounced in the case of the SISID schme. This is due to the fact that the effect of the STO is increased twofold in the process of computing $\Phi_b(m)$, compared to other detectors. More interestingly, the gap between the RCJD scheme and the proposed scheme is reduced by 1 dB for the estimation of the set ID, while a loss of 2 dB is observed when estimating the IFO. It is worth pointing out that the use of the proposed scheme is more favorable for the estimation of the set ID than for the IFO.

Fig. 5 shows the overall probability of detection failure of the detection schemes versus SNR under the same simulation scenarios to Figs. 3 and 4. Immediately, one can see that the trend of the curves is quantitatively similar to that in Fig. 3. Due to its high

susceptibility to STO and fading impairments, the SISID scheme does not work properly in highly dispersive channel condition. More importantly, the SNR loss of the proposed method is less than 1.5 dB in the frequency selective fading channel against the RCJD scheme, while 41.5 % and 70.8 % complexity saving can be obtained over the RCJD and SISID schemes, respectively. Therefore, it can achieve significant complexity saving while experiencing only slight degradation in the detection performance.

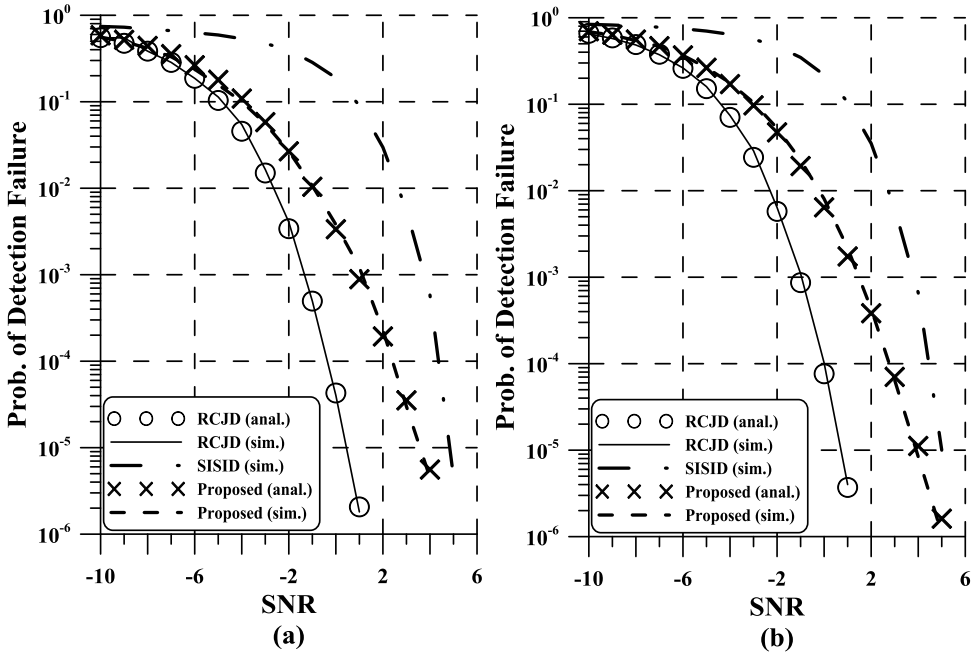

Figure 2: Overall performance of the joint detection schemes versus SNR in the non-fading channel: (a) $M = 1$, (b) $M = 2$

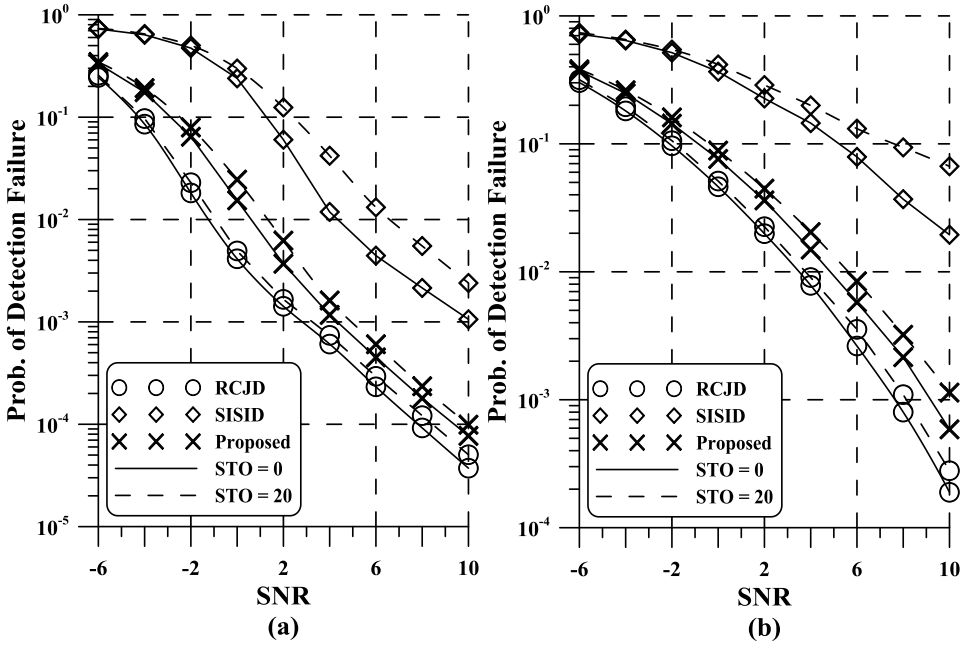

Figure 3: Performance of the IFO detection schemes versus SNR: (a) Pedestrian A, (b) Vehicular A

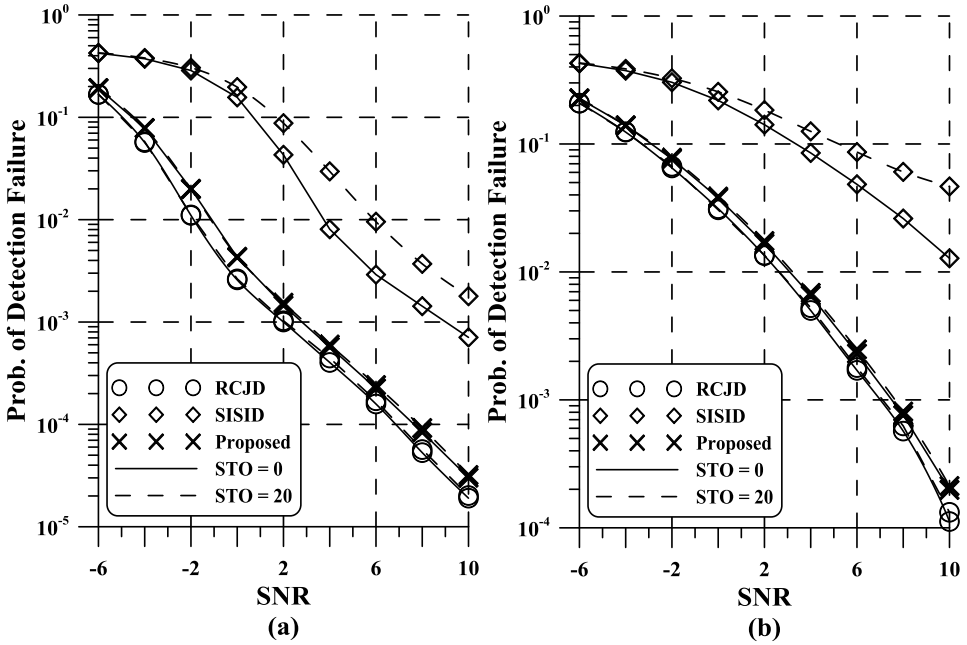

Figure 4: Performance of the set ID detection schemes versus SNR: (a) Pedestrian A, (b) Vehicular A

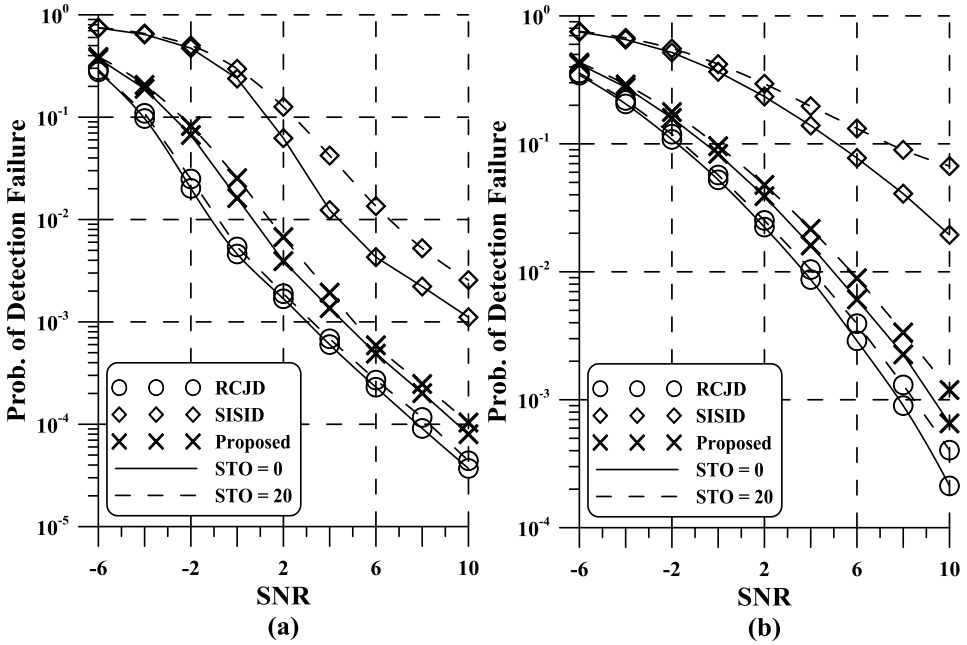

Figure 5: Overall Performance of the joint detection schemes versus SNR: (a) Pedestrian A, (b) Vehicular A

6 Conclusion

To achieve a reliable synchronization in LTE-D2D networks, it is important to perform joint detection of the IFO and set ID with reduced complexity and reliable accuracy. To address this issue, an efficient sequential IFO and set ID estimation scheme is suggested for the LTE sidelink, and it exploits complex conjugate relation between two PSSS sequences. With this conjugate property, the IFO is detected without prior knowledge of the transmitted PSSS, facilitating the reduced-complexity sequential detection. The performance is assessed in terms of theoretical probability of detection failure. It has been verified from simulation results that the proposed sequential detection method has similar performance with significantly low complexity, when compared to existing detection methods.

Acknowledgement: This research was supported by Basic Science Research Program through the National Research Foundation of Korea (NRF) funded by the Ministry of Education (NRF-2018R1D1A1B07048819).

References

3GPP TS36.211 v8.5.0. (2009): *Physical Channels and Modulation*. Release 8; 3GPP, Phoenix, AZ, USA.

Ali, A.; Hamouda, W. (2017): On the cell search and initial synchronization for NB-IoT LTE systems. *IEEE Communications Letters*, vol. 21, no. 8, pp. 1843-1846.

Al-Turjman, F.; Alturjman, S. (2018): Context-sensitive access in industrial Internet of Things (IIoT) healthcare applications. *IEEE Transactions on Industrial Informatics*, vol. 14, no. 6, pp. 2736-2744.

Bao, V. N.; Tuyen, L. P.; Tue, H. H. (2015): A survey on approximations of one-dimensional Gaussian Q-function. *REV Journal on Electronics and Communications*, vol. 5, no. 1-2 , pp. 1-14.

Berggren, F.; Popovic, B. M. (2015): Primary synchronization signal for D2D communications in LTE-Advanced. *IEEE Communications Letters*, vol. 19, no. 7, pp. 1241-1244.

Chu, C. Y.; Lai, I. W.; Lan, Y. Y.; Chiueh, T. D. (2014): Efficient sequential integer CFO and sector identity detection for LTE cell search. *IEEE Wireless Communications Letters*, vol. 3, no. 4, pp. 389-392.

Golnari, A.; Shabany, M.; Nezamalhosseini, A.; Gulak, G. (2015): Design and implementation of time and frequency synchronization in LTE. *IEEE Transactions on Very Large Scale Integration (VLSI) Systems*, vol. 23, no. 12, pp. 2970-2982.

Golub, G. H.; Vanloan, C. F. (1996): *Matrix Computations*. The Johns Hopkins University Press. Baltimore, MA, USA.

Gradshteyn, I. S.; Ryzhik, I. M. (2014): *Table of Integrals, Series, and Products*. Academic Press. Cambridge, MA, USA.

ITU-R Recommendation M.1225. (1997): Guidelines for evaluation of radio transmission technologies for IMT-2000.

Li, S.; Li, S.; Sun, T. (2019): Power allocation for full-duplex NOMA relaying based underlay D2D communications. *KSII Transactions on Internet and Information Systems*, vol. 13, no. 1, pp. 16-33.

Li, X.; Lv, T. (2018): Interference pricing based resource allocation for D2D communications in cellular networks. *KSII Transactions on Internet and Information Systems*, vol. 12, no. 9, pp. 4166-4182.

Li, Y.; Chi, K.; Chen, H.; Wang, Z.; Zhu, Y. (2018): Narrowband internet of things systems with opportunistic D2D communication. *IEEE Internet of Things Journal*, vol. 5, no. 3, pp. 1474-1484.

Morelli, M.; Moretti, M. (2016): A robust maximum likelihood scheme for PSS detection and integer frequency offset recovery in LTE systems. *IEEE Transactions on Wireless Communications*, vol. 15, no. 2, pp. 1353-1363.

Morelli, M.; Moretti, M. (2017): A maximum likelihood approach for SSS detection in LTE systems. *IEEE Transactions on Wireless Communications*, vol. 16, no. 4, pp. 2423-2433.

Myung, J.; Kang, J.; Baek, Y.; Koo, B. (2014): Efficient S-SCH detection algorithm for LTE downlink channel. *IEEE Transactions on Vehicular Technology*, vol. 63, no. 6, pp. 2969-2973.

Nassralla, M. H.; Mansour, M. M.; Jalloul, L. M. A. (2016): A low-complexity detection algorithm for the primary synchronization signal in LTE. *IEEE Transactions on Vehicular Technology*, vol. 65, no. 10, pp. 8751-8757.

Saleem, U.; Jangsher, S.; Qureshi, H. K.; Hassan, S. A. (2018): Joint subcarrier and power allocation in the energy harvesting-aided D2D communication. *IEEE Transactions on Industrial Informatics*, vol. 14, no. 6, pp. 2608-2617.

Sexton, C.; Bodinier, Q.; Farhang, A.; Marchetti, N.; Bader, F. et al. (2018): Enabling asynchronous machine-type D2D communication using multiple waveforms in 5G. *IEEE Internet of Things Journal*, vol. 5, no. 2, pp. 1307-1322.

Sisinni, E.; Saifullah, A.; Han, S.; Jennehag, U.; Gidlund, M. (2018): Industrial internet of things: challenges, opportunities, and directions. *IEEE Transactions on Industrial Informatics*, vol. 14, no. 11 , pp. 4724-4734.

Sriharsha, M.R.; Dama, S.; Kuchi, K. (2017): A complete cell search and synchronization in LTE. *EURASIP Journal on Wireless Communications and Networking*, vol. 101, pp. 1-14.

Tastan, M. (2019): Internet of things based smart energy management for smart home. *KSII Transactions on Internet and Information Systems*, vol. 13, no. 6, pp. 2781-2798.

Wang, L.; Chang, K.; Wang, X.; Wei, Z.; Hu, Q. et al. (2018): A mass-processing simulation framework for resource management in dense 5G-IoT scenarios. *KSII Transactions on Internet and Information Systems*, vol. 12, no. 9, pp. 4122-4143.

Yang, Y.; Zhang, Y.; Dai, L.; Li, J.; Mumtaz, S. et al. (2017): Transmission capacity analysis of relay-assisted device-to-device overlay/underlay communication. *IEEE Transactions on Industrial Informatics*, vol. 13, no. 1, pp. 380-389.

Zhang, Z.; Liu, J.; Long, K. (2012): Low-complexity cell search with fast PSS identification in LTE. *IEEE Transactions on Vehicular Technology*, vol. 61, no. 4, pp. 1719-1729.

Zhao, L.; Wang, H.; Zhong, X. (2019): Interference-aware channel assignment algorithm in D2D overlaying cellular networks. *KSII Transactions on Internet and Information Systems*, vol. 13, no. 4, pp. 1884-1903.

Zhou, L.; Wu, D.; Chen, J.; Dong, Z. (2018): Greening the smart cities: energy-efficient massive content delivery via D2D communications. *IEEE Transactions on Industrial Informatics*, vol. 14, no. 4, pp. 1626-1634.

Zhou, Z.; Dong, M.; Ota, K.; Wang, G.; Yang, L. T. (2016): Energy-efficient resource allocation for D2D communications underlaying cloud-Ranbased LTE-A networks. *IEEE Internet of Things Journal*, vol. 3, no. 3, pp. 428-438.